




# Interaction of antimicrobial peptides with model membranes: a perspective towards new antibiotics

Sanat Karmakar<sup>a</sup> , Surajit Das<sup>b</sup>, and Kalyan Kumar Banerjee<sup>c</sup>

Department of Physics, Jadavpur University, 188, Raja S. C. Mullick Road, Kolkata, West Bengal 700032, India

Received 29 September 2023 / Accepted 22 January 2024

© The Author(s), under exclusive licence to EDP Sciences, Springer-Verlag GmbH Germany, part of Springer Nature 2024

**Abstract** Antimicrobial peptides (AMPs), found in both animals and plants, are used to fend off a wide variety of invading pathogens, such as bacteria, fungi, protozoa, viruses, etc. Their widespread distribution and defensive activity towards all different microbes lead to the successful evolution of complex multicellular organisms. In particular, AMPs target bacterial membranes and disrupt the membrane via the formation of transmembrane pores without interacting with any specific receptors. It is known that different antimicrobial peptides use different mechanisms to disrupt the membrane by forming transmembrane pores. The interaction of the antimicrobial peptide with the membrane depends on peptide charge, hydrophobicity, membrane composition, etc. Therefore, to get insights into the mechanisms of membrane disruption, it is useful to study the model membrane, as biological membranes are complex and regulated by various other proteins, cholesterol, etc. In the present review, we will primarily describe the interaction of antimicrobial peptides with phospholipid membranes, which mimic the bacterial membrane, in view of understanding the mechanism of action, various factors affecting their activity, application prospects in drug therapeutics, etc.

## 1 Introduction

Antimicrobial peptides (AMPs) are a diverse group of molecules that are evolutionarily conserved components of the innate immune response in the animal and human body against invading pathogens, such as viruses, fungi, bacteria, protozoa, etc [1, 2]. Prolonged use of conventional antibiotics leads to resistance to the spectrum of bacteria and other invading pathogens. Hence, there is an urgent need for alternatives to the common antibiotics [3]. Therefore, the current research focuses on the development of novel methods to get rid of the inevitable resistance that develops with conventional antibiotics [4–6]. A large number of recent studies have suggested that AMPs have the potential to act as excellent antibiotic toward a broad-spectrum of Gram-positive and Gram-negative bacteria [7]. The unique mode of action with less bacterial resistance than conventional antibiotics has led to a new possibility in the development of AMPs as human therapeutics [8].

A total of 3569 antimicrobial peptides have been reported in the Antimicrobial Peptide Database (<https://aps.unmc.edu>). AMPs mostly contain 10–60 amino acid residues. Almost all of them are cationic, and a few AMPs are found to be anionic in nature [9]. AMPs, which are a unique and diverse group of molecules found in bacteriolytic substances, basic antimicrobial proteins, and basic linear tissue polypeptides, are classified on the basis of their source, amino acid composition, structural characteristics, such as size, sequence, charge, conformation and structure, hydrophobicity, amphipathicity, etc. [1, 7]. Classes of AMPs are summarised in Table 1 [1]. In the present review, we are not elucidating the details of the various classes of AMP. However, some details can be found in Ref. [1] and references therein. Current research focuses on host-derived antimicrobial molecules, particularly antimicrobial fragments of large proteins, which are identified as possible alternatives to therapeutics for the treatment of antibiotic-resistant bacterial infections [10, 11].

AMP-mediated cell killing may be rapid or may take several minutes ( $\sim 15$ – $90$  min). Further, different AMPs use different mechanisms to destroy cellular integrity. It is extremely difficult and technically challenging to unravel

<sup>a</sup> e-mail: [sanat.karmakar@jadavpuruniversity.in](mailto:sanat.karmakar@jadavpuruniversity.in) (corresponding author)

<sup>b</sup> e-mail: [surajitphys@gmail.com](mailto:surajitphys@gmail.com)

<sup>c</sup> e-mail: [kalyanbanerjee802@gmail.com](mailto:kalyanbanerjee802@gmail.com)

the mechanisms or process of cell death due to the complexity of the membrane [12]. Therefore, it is often useful to study model membranes to get insights into the mechanisms of antimicrobial activity. Antimicrobial action initiates due to the attraction of cationic peptides towards negatively charged bacterial membranes, primarily through electrostatic attraction. Peptides then associate and embed into the head group regions parallel to the membrane surface (S-state). With increasing peptide concentration, the orientation of the peptides becomes perpendicular to the membrane surface (I state) to form transmembrane pores and finally disrupt the membrane. All these steps preceding cell death, i.e., antimicrobial activity, can be studied using a model membrane. Phospholipids, especially anionic lipids such as phosphatidylglycerol (PG) and phosphatidylserine (PS), would be appropriate to use as bacterial surfaces are negatively charged. In this review, we shall discuss the interaction of various antimicrobial peptides with the model membrane and their pore-forming activity. As model membranes, large and small unilamellar vesicles (LUV, SUV), multilamellar vesicles (MLV), lamellar phase, oriented stack of bilayers, etc. were mainly used to study the interaction of AMPs with the membranes. However, owing to their large size, giant unilamellar vesicles (GUV) were employed to directly visualise the evidence of pore formation. Unilamellar vesicles can be prepared using some standard techniques described in the literature. For example, the extrusion method is widely used to prepare LUV (diameter  $\sim$  100–200 nm) and SUV (diameter  $<$  100 nm) [13]. SUVs can also be prepared using an ultrasonic bath or probe sonicator. On the other hand, electroformation is a popularly used technique to produce giant unilamellar vesicles of size 5–100  $\mu$ m [14]. A variety of experimental as well as theoretical techniques have been employed to study the interaction of AMPs with model membranes. The effects of AMPs on the structure and integrity of the membranes were investigated using X-ray crystallography [15–17], NMR spectroscopy [18, 19], Fourier transform infrared (FTIR) [20], Raman, fluorescence or CD optical, and other spectroscopic studies [21–26]. Interaction, binding affinity of specific AMP with the different composition of the membranes, as well as thermodynamics of binding kinetics, were studied using fluorescence spectroscopy, zeta potential, dynamic light scattering (DLS), differential scanning calorimetry (DSC), and isothermal titration calorimetry (ITC) [27–33]. The structure of pores was studied using neutron scattering and interface-sensitive x-ray scattering [34]. Optical microscopy, which includes phase contrast microscopy, fluorescence microscopy, laser scanning confocal, etc., was employed to observe the morphology of the giant unilamellar vesicles when exposed to AMPs in an aqueous medium, which eventually provided evidence of pores as well as the kinetics of the pore formation process [35–39]. Besides experimental studies, molecular dynamic simulation studies have also been attempted to get insights into the molecular selectivity of AMPs, the dynamics of counter-ion release upon adsorption of AMPs on the membrane, and the molecular basis of antimicrobial activity [40–42]. The interaction of AMPs with the model membrane and mechanisms of antimicrobial activity in light of all these experimental techniques mentioned will be delineated in detail in this review. Possible proposed mechanisms of antimicrobial activity reported in the literature will be discussed. Finally, the recent development of AMPs to be used as emerging materials for the replacement of conventional antibiotics will be discussed.

## 2 Interaction of AMP with phospholipid membranes

Studies on the interaction of AMP with phospholipids are essential to obtain insights into membrane selectivity and other factors that are strongly dependent on antimicrobial activity. Adsorption of cationic peptides on the negatively charged membrane primarily involves electrostatic attraction. Therefore, zeta potential would be an appropriate technique to look at the propensity of AMP to the membrane, which may be electrostatically driven. A systematic investigation of the interaction of an antimicrobial peptide NK-2 with model membranes composed of both negatively charged lipids, such as 2-dioleoyl-sn-glycero-3-phosphocholine (DOPG), palmitoyloleoyl PG (POPG), 2-dimyristoyl-sn-glycero-3-phosphoglycerol, sodium salt (DMPG), and zwitterionic lipids, such as 2-oleoyl-1-palmitoyl-sn-glycero-3-phosphocholine (POPC), 1,2-dioleoylphosphatidylcholine (DOPC), 1,2-dimyristoyl-sn-glycero-3-phosphocholine (DMPC), 1,2-palmitoyl-sn-glycero-3-phosphocholine (DPPC), etc., showed strong binding affinity towards the negatively charged membrane as revealed by zeta potential and dynamic light scattering [31, 33, 43]. It is important to mention here that phosphatidylethanolamine (PE) and PG are the most abundant phospholipids present on the bacterial cell surface [31]. Therefore, stronger affinity towards the PG and PE-PG membranes and much weaker affinity towards PC, which is a major constituent of the eukaryotic cell membrane will enable AMPs to be used as potential candidates for drug therapeutics. Figure 1 shows the binding affinity of NK-2 towards membranes with various compositions [33, 43]. It is clearly evident from the figure that charge neutralisation of negatively charged vesicles occurs at a much higher NK-2 to lipid ratio (1:5) than that of neutral vesicles (1:250). Interestingly, saturation of the zeta value, i.e., overcharge compensation, occurs at different zeta values for different lipids, suggesting significant entropic contributions in the membrane peptide interaction. Similar results were obtained for the membrane composed of POPG, DMPG [31] and POPE/POPG mixtures for another AMP Chex1-Arg20 [43]. However, NK-2 and Chex1-Arg20 do not interact with unsaturated DOPC, POPC, or saturated phospholipid DPPC. This is desirable as they are major constituents of the eukaryotic plasma

**Table 1** Classification of antimicrobial peptides

Classes of antimicrobial peptides	Examples
Anionic peptide	Maximin H5 from amphibians Small anionic peptides rich in glutamic and aspartic acids from sheep, cattle and humans Dermcidin from humans
Linear cationic $\alpha$ helical peptides	Cecropins (A), andropin, moricin, ceratotoxin and melittin from insects Cecropin P1 from <i>Ascaris</i> nematodes NK-2 from NK-lysin, bovine branin Magainin (2), dermaseptin, bombinin, brevinin-1, esculentins and buforin II from amphibians Pleurocidin from skin mucous secretions of the winter flounder Seminalplasmin, BMAP, SMAP (SMAP29, ovispirin), PMAP from cattle, sheep and pigs LL37 from humans
Cationic peptides enriched for specific amino acids	Proline-containing peptides include abaecin from honeybees Proline- and arginine-containing peptides include apidaecins from honeybees drosocin from <i>Drosophila</i> ; pyrrococin from the European sap-sucking bug bactenecins from cattle (Bac7), sheep, and goats and PR-39 from pigs Proline- and phenylalanine-containing peptides include prophenin from pigs Glycine-containing peptides include hymenoptaecin from honeybees Glycine- and proline-containing peptides include coleopteracin and holotricin from beetles Tryptophan-containing peptides include indolicidin from cattle Small histidine-rich salivary polypeptides, including the histatins from man and some higher primates
Anionic & cationic peptides that contain cysteine and form disulphide bonds	Peptides with 1 disulphide bond include brevinins Peptides with 2 disulphide bonds include protegrin from pigs and tachyplesins from horseshoe crabs Peptides with 3 disulphide bonds include $\alpha$ defensins from humans (HNP-1, HNP-2, cryptidins), rabbits (NP-1) and rats; $\beta$ defensins from humans (HBD1, DEFB118), cattle, mice, rats, pigs, goats and poultry; and rhesus $\theta$ -defensin (RTD-1) from the rhesus monkey Insect defensins (defensin A) SPAG11/isoform HE2C, an atypical anionic $\beta$ -defensin Peptides with > 3 disulphide bonds include drosomycin in fruit flies and plant antifungal defensins form disulphide bonds
Anionic and cationic peptide fragments of larger proteins	Lactoferricin from lactoferrin. Casocidin I from human case Antimicrobial domains from bovine $\alpha$ -lactalbumin, human haemoglobin, lysozyme and ovalbumin

The mode of bacteria killing for most of the peptides is given in Ref. [1]

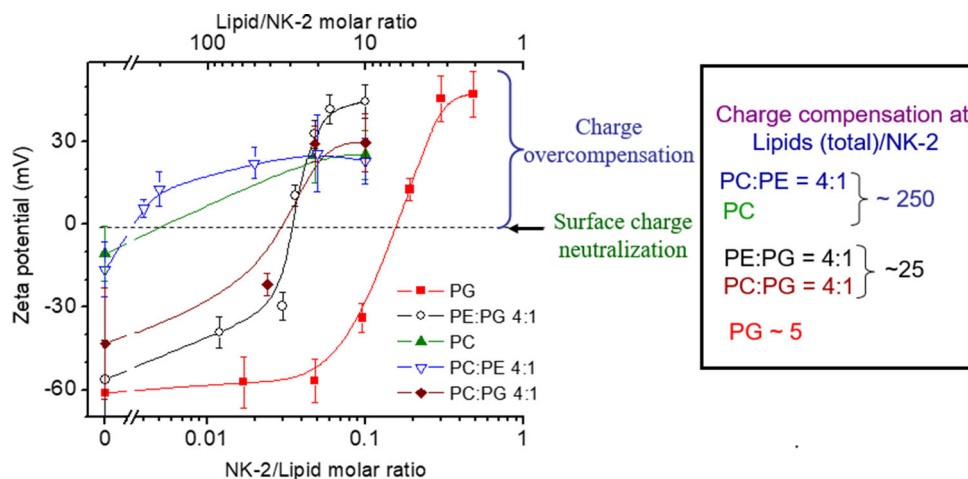


**Fig. 1** Zeta potential of LUV made from various phospholipid compositions as indicated in the figure legend for various NK-2 to lipid molar ratios. Charge compensation at the lipid-to-NK-2 ratio for various lipid compositions is also shown [33]

membrane. A theoretical description of the interaction using maximal and minimal values of zeta potential has been used to estimate the binding free energy, membrane surface charge, and effective peptide charge [35].

The DLS technique, in principle, shows evidence of membrane-membrane interaction induced by AMPs. Karmakar et al. have shown that the average size of LUV increases with an increase in peptide concentration. Extensive aggregation was also found in cationic antimicrobial polynorbornenes without complete membrane disintegration [44]. Proliferation of average size suggests aggregation of vesicles mediated by AMP [31]. The unstable LUV and aggregation phenomena can also be envisaged from the correlation curve of the DLS measurement. Cationic antimicrobial peptide Chex1-Arg20 also induces aggregation of LUV made from negatively charged POPE:POPG (7:3) at a higher peptide-to-lipid ratio, and no such aggregation was found in the POPC membrane [44]. Differential scanning calorimetry study showed decrease in the main phase transition temperature of negatively charged lipids (DMPG, DMPS, and DMPA, etc.) with increasing peptide concentration [43]. However, the effect of two small peptides (Ac-RW and C-RW) on the phase transition of zwitterionic lipid is not significant [43]. This result suggests that AMPs showed higher selectivity towards negatively charged membranes. The reduction in transition temperature was due to the perturbing effect of the lipid chain, which overcompensates the electrostatic effect between the cationic peptide and the negatively charged phospholipid (see Ref. [43] and references therein). The effect of AMP on the phase transition of the lipid bilayer was not studied for unsaturated lipids, as the chain melting transition of unsaturated lipids is very low ( $-18\text{ }^{\circ}\text{C}$  for DOPC) [45].

Spectroscopic techniques, such as NMR and FTIR, have been used to study the effects of nonselective  $\alpha$ -helical and selective intermolecular  $\beta$ -sheet peptides on DMPG and DMPC multilamellar vesicles [20].  $^{31}\text{P}$  NMR reveals that peptides interact with the head group of DMPC and DMPG bilayers. However,  $^2\text{H}$  NMR and Fourier transform infrared suggested an ordering of the hydrophobic core of bilayers at the onset of pore formation. The effect of acyl chain ordering has also been investigated using FTIR [20]. Solid-state NMR spectroscopy has shown that AMPs, like magainins or derivatives exhibit antimicrobial activities when their  $\alpha$ -helix conformation is oriented parallel to the bilayer surface [18, 19]. A review of various solid-state NMR spectroscopy study on cationic amphipathic peptides reconstituted in an oriented bilayer to obtain insights into the structure, dynamics and topology of the membrane-associated polypeptides was presented in Ref. [18] and references therein. Another spectroscopic method circular dichroism (CD) and oriented circular dichroism (OCD) have widely been employed to reveal the conformational change of AMPs in the presence of membrane. CD studies have shown that cationic amphipathic peptides, such as magainin 2, NK-2, cecropins, mellitin, and alamethicin adopt random coil unstructured conformation in an aqueous solution, but changes to stable  $\alpha$  helix when exposed to membrane or other self assembled structure by amphiphiles [21, 24, 26, 32]. This is indeed a requirement for an AMP to form pores, as  $\alpha$  helix conformation is needed for peptide insertion into the membrane. For high lipid-to-peptide ratio, i.e. at a low peptide concentration, a helical axis of the peptide aligns parallel to the membrane surface (S-state) and peptide undergoes dynamic reorientation perpendicular to the membrane surface on increasing peptide concentration and eventually complete destruction (micellization) occurs [46]. Such conformational and the orientational change were also confirmed by solid-state NMR mentioned before.

The hydrophobicity of an AMP is defined as the percent of hydrophobic residues such as valine, leucine, isoleucine, alanine, methionine, phenylalanine, and tyrosine and tryptophan in the peptide sequence. The hydrophobicity of AMPs indicates the ability of AMP to partition into the lipid bilayer of the membrane. It has been established in the literature that peptides with greater hydrophobicity, typically  $> 50\%$  can penetrate the hydrocarbon

region of the lipid bilayer and exhibit antimicrobial activity. Further, excessive levels of hydrophobicity of the peptides may lead to cytotoxicity, hemolytic and even loss of antimicrobial activity [47–49]. Chen et al. have shown the relationship between hydrophobicity and the antimicrobial and hemolytic activities of the peptide analogue  $V13K_L$  [47] by changing the level of hydrophobicity. Studies revealed a two-fold effect of hydrophobicity on the peptide's antimicrobial activity. An increase in peptide hydrophobicity from a very low level caused an enhancement in antimicrobial activity until an optimal hydrophobicity was reached. A further increase in hydrophobicity beyond the optimum antimicrobial activity was weakened dramatically, resulting in a loss of antimicrobial activity for the peptide. The effect of hydrophobicity on the antimicrobial activity of different peptides can be found in Ref. [49]. Peptide hydrophobicity was found to affect the rate of pore formation, pore size, and stability of pores. The mode of action was also found to be dependent on the position of the hydrophobic amino acid in the peptide sequence [50].

## 2.1 Thermodynamics of binding kinetics

Thermodynamics of binding kinetics of AMPs have been widely studied using isothermal titration calorimetry (ITC). A detailed technique along with its applications can be found in a recent review article [51]. In this technique, heat produced (exothermic) or absorbed (endothermic) as a result of the interaction of peptides with lipid vesicles was measured. Isothermal titration calorimetry provides the binding constant and the binding enthalpy by measuring the heat of the reaction due to the interaction of AMPs with the vesicles. Each injection produces a characteristic heat signal arising from either an exothermic or endothermic reaction. The heat of dilution was measured by injecting either lipid vesicles into the peptide or titrating peptides into lipid vesicles. The former procedure is more appropriate because it provides significant heat at each injection, as a higher concentration of titrant is required to fill the syringe in ITC measurement [51]. The net heat per injection was obtained by the heat of dilution. Now, integrating the heat at every injection provides us with the binding isotherm for the peptide. Many of the earlier studies have shown an exothermic heat signal followed by a weak endothermic signal upon peptide into lipid (LUV or SUV) titration [28, 52, 53]. However, Gabriel et al. have found only endothermic heat signals when titrating polymers into LUV, and interestingly, Karmakar et al. have seen a few exothermic heat signals in between two endothermic responses. All these different behaviours of heat signals might have important consequences in view of their mechanisms of action towards the membranes. The electrostatic contribution of the peptide-membrane interaction usually leads to exothermic heat. However, endothermic responses are entropy-driven and are assigned to pore formation [52]. It is important to mention that heat contribution also comes from the conformational and orientational changes of peptides upon interaction with membranes, as well as the release of water molecules at the membrane-water interface due to peptide binding.

The partition model is widely used to fit the binding isotherm. The partition model assumes the extent of peptide binding,  $X_b$ , per mole of lipid is related to the apparent binding constant via the relation  $X_b = K_{app}C_f$ .  $C_f$  is the free peptide constant in the solution. It is important to mention that  $K_{app}$  does not remain constant but rather changes with the free peptide concentration. This is due to the fact that when cationic peptides adsorb, the membrane gets positively charged, and hence further adsorption of cationic peptides is restricted due to electrostatic repulsion. Therefore, the intrinsic binding constant ( $K_{int}$ ) would be the most relevant parameter, which is directly proportional to the concentration of the peptide in the vicinity of the membrane ( $X_b = K_{int}C_M$ ).  $C_M$  being the intrinsic concentration of the peptide. This model essentially includes an electrostatic contribution to the binding, and hence  $C_M$  to be determined from the Boltzmann distribution.  $C_M = C_f e^{-\frac{z_p F \psi_0}{RT}}$ .  $z_p$  is the effective peptide charge, which can be obtained from the theory described in ref. [35].  $F$  and  $\psi_0$  are the Faraday constant and surface potential, respectively.  $RT$  is the thermal energy. Each pair of  $X_b$  and  $C_f$  obtained from experimental binding isotherms, the numerical solution of the binding constant ( $K$ ),  $\psi_0$  and  $C_M$  were estimated. In an ITC experiment (lipids into peptide injection), the  $X_b$  and the enthalpy change  $\Delta H$  per mole of peptides can be measured directly. Further, the Gibbs energy and the entropy contribution were determined from the thermodynamic relation  $\Delta G = -RT \ln(55.5K) = \Delta H - T\Delta S$ . Here, the concentration of water (55.5 M) was used to correct the unit of  $K$  to the molar fraction [28, 33]. Thermodynamic parameters of binding kinetics are summarised in table 2.

## 2.2 Process of pore formation: membrane tension and membrane thinning effect

It was known that melittin induces stable transmembrane pores in both anionic and zwitterionic vesicles without disintegrating membranes [54, 55]. When the membrane is subjected to external stress, such as by applying lateral membrane tension, transmembrane pores are formed before the membrane gets ruptured [56]. The increase in membrane tension prior to pore formation and rupture or disintegration of the membrane is an essential requirement. As AMPs are able to induce pores, it is conceivable that AMPs can generate membrane tension, similar to that of mechanical stress. This function of AMP was illustrated using micropipette aspiration with GUV, x-ray diffraction with fully hydrated oriented multilayers, and OCD [26, 38, 54]. Let us first discuss the



**Table 2** Thermodynamic parameters of peptide-membrane interaction

Lipids	Peptides	$K(M^{-1})$	$\Delta H$ (kcal/mol)	$\Delta G$ (kcal/mol)	$T\Delta S$ (kcal/mol)	$z_p(e)$	References
POPC/POPG	PGLa	1500	-12.3	-6.8	-5.4	+4.6	[52]
DOPG	NK-2	$2.5 \times 10^8$	0.8	-13.8	14.6	6.6	[33, 35]
DOPC/DOPG	NK-2	$7.3 \times 10^8$	2.9	-11.7	14.4	7	[33, 35]
POPE/POPG	Polynorbornenes	-	36	-10.8	46.8	-	[44]
POPC/POPG	Nisin Z	1.8	- 8.5	-	-	3.5	[28], references therein
POPC/POPG	Cinnamycin	$7 \times 10^7$	-8.5	-10.7	-	-	[28], references therein
POPC/POPG	Magainin 2	55	-17.1	-4.8	-	3.7	[29]

$K$  binding constant,  $\Delta H$  enthalpy change,  $\Delta S$  entropy change,  $z_p$  effective peptide charge

membrane-thinning effect of AMPs, melittin, and alamethicin, as seen from the x-ray diffraction results. The equilibrium bilayer thickness can be estimated from the average phosphate peak-to-phosphate peak distance of the electron density profile (Fig. 2a) obtained from the XRD of fully hydrated oriented multilayers of DOPC/DOPG mixture for various peptide-to-lipid ( $P/L$ ) ratios [38, 54]. Bilayer thickness decreases (membrane thinning) with increasing  $P/L$  ratio and above a threshold  $P/L^*$  (1/70 for melittin/di20:1 PC, 1/39 for melittin di22:1 PC, 1/45 for melittin/DOPC/DOPG), but membrane thickness does not change significantly. Interestingly, for  $P/L < P/L^*$ , orientation of peptides is found to be parallel to the membrane surface, whereas for  $P/L > P/L^*$ , peptides change their orientation to being perpendicular to the membrane. The correlation between the bilayer thinning and the change in peptide orientation has also been seen for other antimicrobial peptides in many different lipid compositions [26, 57]. However, the value of  $P/L^*$  and the degree of membrane thinning change with peptide and lipid composition. Later, Lee et al. showed that at  $P/L = P/L^*$ , the onset of pore formation begins (as well as the onset of membrane thinning plateau formation). The membrane thinning is the consequence of increasing membrane tension. Therefore, these results clearly suggest that an increase in membrane tension as well as a change in peptide orientation are essential requirements in the process of pore formation.

As discussed, the threshold peptide-to-lipid ratio ( $P/L^*$ ) changes when membranes are prepared from different lipids (di22:1 PC and di22:1 PC) [54]. Further, Gidalevitz et al. have reported that the AMP protegrin interacts with the membrane in a manner that strongly depends on the membrane lipid compositions [17]. Molecular dynamic simulation has shown that the lipid compositions (DMPC and DPPC) affect the peptide-induced membrane thinning [58]. They have shown that the local membrane thinning is dependent on the orientation of the peptide within the bilayer membrane. Therefore, the peptide-induced membrane thinning may be a common feature, but the initiation of the plateau region, indicating the onset of pore formation, depends on the lipid composition of the membrane.

In micropipette aspiration on GUV, Lee et al. have shown a linear increase in membrane area with peptide binding before pore formation, which complements the results on membrane thinning, which is also proportional to  $P/L$  [38]. In the micropipette experiment, GUV is aspirated using a micropipette, and the relative increase in membrane area ( $\frac{\Delta A}{A}$ ) was estimated by measuring the length ( $L_p$ ) of the protrusion inside the micropipette under constant tension. Responses of GUV exposed to melittin were monitored using confocal fluorescence microscopy, and fluorescence micrographs of the surface of the GUV with time were recorded. From the images of GUV (see the schematic diagram, Fig. 2b), area and volume change can be determined from the relations  $\Delta A = 2\pi R_p \Delta L_p + 8\pi R_v \Delta R_v$  and  $\Delta V = \pi R_p^2 \Delta L_p + 4\pi R_v^2 \Delta R_v$ , respectively. Symbols are depicted in Fig. 2b. If there is no leakage and no osmotic stress between the interior and exterior of the GUV, the volume of the GUV remains unaltered. Further, the change in the radius of the vesicles is too small to measure. Therefore, one assumes  $\Delta V = 0$ , and hence  $\Delta A$  is directly proportional to  $\Delta L_p$ . This measurement and analysis are applicable and true before the pore formation of GUV induced by AMP. This experiment again indicates that peptides increase membrane tension before molecular leakage, similar to that found in the micropipette experiments with increasing tension without being exposed to peptides [59].

Pores in the membrane are always produced under tension, and the stability of the pores depends on the interplay between a membrane tension ( $\sigma$ ) which tends to enlarge the pore, and a line tension ( $\gamma$ ) which tends to close the pore. If the pore is assumed to be circular of radius  $R$ , the energy associated with a pore is given by  $E_{\text{pore}} = 2\pi R\gamma - \pi R^2\sigma$  [26]. Equilibrium radius of the pore radius  $R^* = \frac{\gamma}{\sigma}$ . If  $R > R^*$ , pores expand until vesicle rupture, whereas for  $R < R^*$ , pores close [60]. Peptide binding to the membrane also renders membrane tension, as evidenced by the micropipette aspiration of GUV and the membrane thinning effect of bilayer stacks. Upon insertion of the peptide into the bilayer, an additional area is introduced in the membrane head group regions

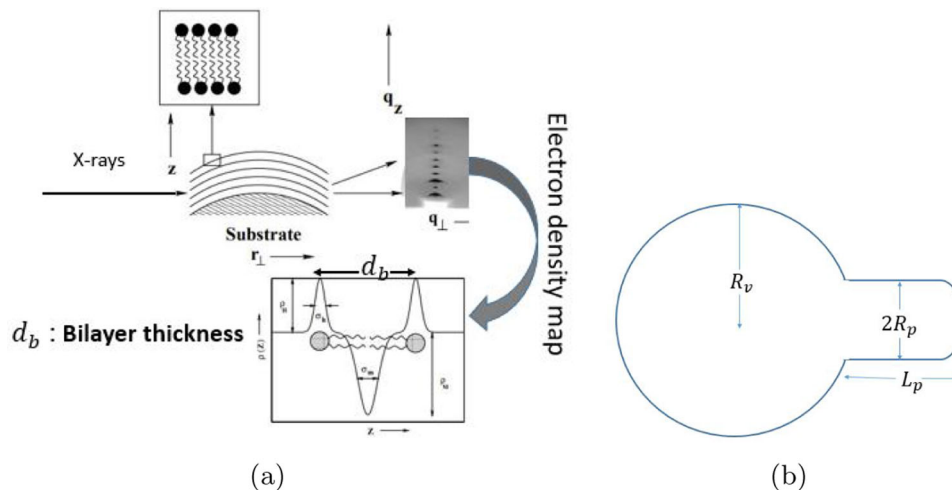


**Fig. 2** **a** Schematic diagram of the experimental procedure for small angle x-ray diffraction for an oriented stack of bilayers. A typical electron density map is shown for three Gaussian model, two with amplitude  $\rho_H$  for the phosphate head group and one with negative amplitude ( $\rho_M$ ) for the hydrocarbon chain region. The widths of the Gaussian for both regions are also shown in the figure. Bilayer periodicity  $d = d_b + d_w$ , where  $d_b$  and  $d_w$  are the bilayer thickness and water layer thickness, respectively. Therefore, bilayer  $d_b$  was measured from the peak to peak distance from the transbilayer electron density profile, as shown **(b)**. Schematic diagram of the micropipette aspiration of GUV.  $L_p$  is the length of the protrusion inside the micropipette.  $R_v$  and  $R_p$  being the radii of GUV and micropipette, respectively. The volume and area of the GUV can be estimated from this diagram

(for example, melittin adds an area of  $3 \text{ nm}^2$ ) and thus causes a local deformation in the monolayer. A detailed theoretical description of pore formation and pore dynamics that is consistent with the experimental results on micropipette aspiration of GUV and x-ray/neutron scattering of oriented bilayer stacks is presented in Ref. [60] (references therein).

### 3 Evidence of transmembrane pores induced by AMPs

It has been reported by Lee et al. that transmembrane pores form beyond the threshold or critical value of  $P/L$ , i.e.,  $P/L > P/L^*$ , indicated by the plateau region of membrane thickness. There are two types of experimental approaches that have been described in the literature to show evidence of transmembrane pores. (i) Fluorescence confocal microscopy and fluorescence spectroscopy, which show the leakage of calcein or other fluorescence probes entrapped within the vesicles. (ii) Optical microscopy approach, mainly phase contrast microscopy. First, we discuss the study based on fluorescence and then the phase contrast microscopy approach.

#### 3.1 Membrane permeabilization assay: fluorescent leakage experiment

The loss of fluorescence intensity of fluorescence dye TRsc (625 Mr) encapsulated in GUV made from DOPC/DOPG (7:3) was measured with time [38]. Within the time scale of 400 s, photobleaching was assumed to be negligible. Therefore, the reduction in fluorescence intensity is due to the leakage of dye through transmembrane pores. Another widely used calcein release fluorescence assay is employed to measure the extent of membrane permeabilization or leakage induced by AMPs [61–64]. In this assay, calcein-loaded LUV (PC/PG) was exposed to AMP, and fluorescence intensity as a function of time was measured. The enhancement of fluorescence intensity due to the release of calcein indicates the presence of transmembrane pores. Fluorescence intensity due to leakage of calcein-loaded LUV/SUV was normalised relative to the total fluorescence intensity ( $I_T$ ), measured after complete disruption of all the vesicles by Triton X-100. The percentage of released calcein is estimated using the equation: % of calcein released =  $\frac{I_F - I_B}{I_T - I_B} \times 100\%$ , where  $I_F$  and  $I_B$  are the fluorescence intensities after and before peptide addition. Oñate-Garzón et al. have shown that calcein-loaded SUVs prepared from Gram-negative bacteria mimicking lipids, both the neutral and cationic peptides, show activity on POPG SUVs, with  $\sim 85\%$  of the calcein released at a peptide-to-lipid ratio of 1:100 [63]. The permeabilization activity of SUVs with different membrane compositions when exposed to cationic peptides decreases according to the following order: POPG > POPC/POPG > POPC > POPE/POPG. It is important to mention that the pore size must be larger than the size of the calcein molecules.

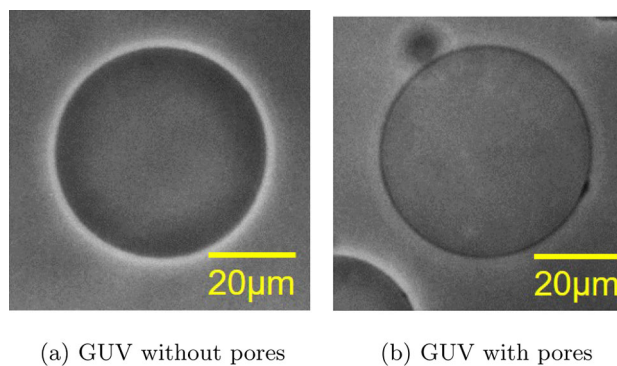


**Fig. 3** **a** GUV shows a halo region due to the refractive index contrast between the interior (sucrose) and exterior (glucose) of the vesicle. The same concentration of glucose and sucrose was used to avoid any resultant osmotic stress between the interior and exterior of the GUV. **b** GUV, when exposed to the antimicrobial peptide NK-2, exhibits leakage of the internal fluid through the transmembrane pores induced by NK-2, and hence the contrast between inside and outside the GUV is lost

enabling their translocation from the interior of the vesicle through pores. The calcein leakage from anionic vesicles was in agreement with the MARTINI simulation [64].

### 3.2 Phase contrast and fluorescence microscopy

Phase contrast microscopy on GUV composed of DOPC/DOPG (4:1) has been employed to visualise directly the antimicrobial activity of the antimicrobial peptide NK-2 [34]. This technique has gained importance as no fluorescence dyes were incorporated in GUV, which may affect the properties of the membrane. As shown in Fig. 3a, a halo region appears in the phase contrast micrograph of GUV due to a mismatch in the refraction indices of the interior and exterior of the vesicles. When GUV is exposed to NK-2, pores are formed. Therefore, the leakage of internal fluid is expected through the pores. The halo region, which results in a contrast in the intensity grey value across the halo, is expected to disappear with time (contrast loss) due to the exchange of fluid when there are pores in the membrane. Therefore, porated vesicles should look similar to those without any contrast between the interior and exterior of GUV, i.e., without diluting with glucose (Fig. 3b). The pores are large enough to permeate the sucrose and glucose molecules and fluids between the interior and exterior of the GUV. The time scale of pore fluctuations is also assumed to be much faster than the rate of diffusion of glucose or sucrose molecules. Therefore, pores are not transient but stable, as the contrast loss across the halo region of GUV remains stable with time. GUVs made from DOPC do not show a significant decrease in  $I_{\text{ptp}}$  in the presence of NK-2, suggesting NK-2 does not form pores on neutral or zwitterionic membranes. Such behaviour is due to the very weak binding affinity of NK-2 towards PC, as seen from the zeta potential. Anionic GUV, exposed to Magainin 2, a well-established pore-forming peptide, also shows similar contrast loss across the halo region of their phase contrast micrographs [35].

The kinetics of pore formation can be described by the decrease in the intensity grey value across the halo regions. Figure 4 depicts the procedure to calculate peak-to-peak intensity ( $I_{\text{ptp}}$ ) across the halo from the phase contrast image of GUV [35].  $I_{\text{ptp}}$  as a function of time was obtained by measuring the grey value of the peak to peak of line profiles across the GUV (Fig. 4). The decrease or decay of  $I_{\text{ptp}}$  with time was then fitted to a single exponential decay curve to determine the rate constant of the pore-forming kinetics. The progressive decrease in intensity was also observed in fluorescence images of calcein-loaded GUV. The calcein leakage leads to a progressive decrease in the calcein concentration inside the GUV after the addition of magainin 2 [65].

### 3.3 Evidence of pores in bacterial membranes

It is now desirable and relevant to discuss the antimicrobial peptide-induced pore formation in bacterial cell surface. A review on the pore former antimicrobial peptides and their actions on invading pathogens were reported by Brogden et al. [1]. Time-resolved AFM images along with scanning electron microscopy have shown that the antimicrobial peptide caerin caused localised defects in the cell membrane of lysed *K. pneumonia* [66]. These defects eventually transformed into large pores before the membrane was destroyed. The evidence of membrane damage was visualised by cryo-EM at the concentration used in AFM experiments. These experimental studies clearly support the pore-forming mechanism of action of antimicrobial peptides. Attila Farkas et al. have reported the disruption of the integrity of the membrane of two foodborne pathogens, *Salmonella enterica* and *Listeria monocytogenes*, by antibacterial peptides such as NCR247, NCR335, polymyxin B (PMB), and streptomycin



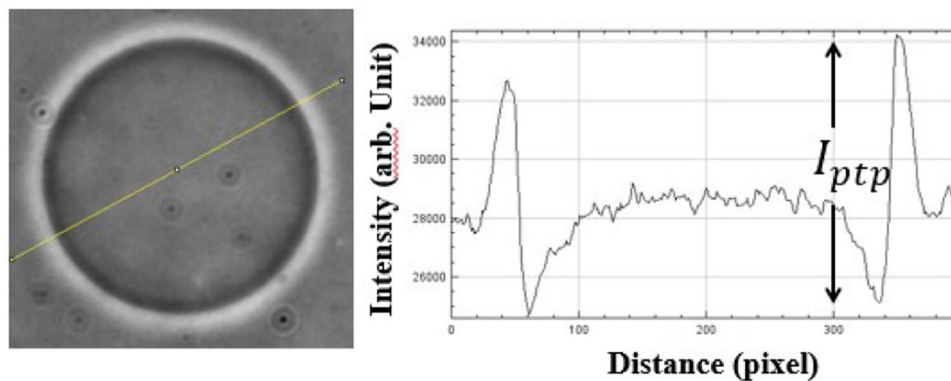


**Fig. 4** Determination of the peak-to-peak intensity (grey value),  $I_{ptp}$ , across the halo region of the phase contrast micrograph of GUV [35] Analysis of GUV images has been performed using ImageJ software

[67]. Fluorescence confocal microscopy and scanning electron microscopy studies revealed that both NCRs interacted with the bacteria, leading to pore formation and hence cell death. Recently, high-resolution cryoelectron tomography (cryo-ET) and high-speed atomic force microscopy (HSAFM) enabled us to directly visualise the pepD2M-induced disruption of the outer and inner membranes of the Gram-negative bacterium *Escherichia coli* [68]. Further, Chen et al. have shown that pepD2M disrupts the *E. coli* membrane using a carpet/detergent-like mechanism, similarly to that found with a well-known pore-forming peptide, melittin [68].

### 3.4 Kinetics of pore formation

To reveal the mechanisms of antimicrobial activity, the kinetic pathway of pore formation in membranes induced by AMPs is necessary to elucidate. The kinetics of pore formation depend on the size of the GUV [69] as well as the spontaneous curvature of the membrane [16] (references therein). Further, the time scale of the process is also dependent on the peptide concentration [70]. All these parameters, affecting pore-forming kinetics, may vary from one GUV to another. Therefore, different GUVs seem to take different times to initiate pore formation. In the experiments discussed in Refs. [35, 62], the average responses of GUV exposed to peptide were monitored, and hence the determination of a precise time point to initiate pore formation for individual vesicles at different peptide concentrations is not possible. However, the rate constant ( $\tau$ ) for different peptide concentrations was unambiguously determined from the fit to the decay curve mentioned in the earlier section. Tamba et al. have investigated the rate of leakage of different-sized fluorescent probes through the magainin 2-induced pores in single GUVs composed of DOPC/DOPG (1:1). They showed that magainin-induced leakage of fluorescence probes such as Texas-Red dextran 10000 (TRD-10k), Texas-Red dextran 3000 (TDR-3k), and Alexa-Fluor trypsin inhibitor occurred in two stages: a transient rapid leakage in the initial stage followed by a stage of slow leakage [69]. They suggested that magainin 2 initially induces a large, transient pore in lipid membranes in which decay is much faster (4  $\mu\text{M}$  Magainin 2/calcein,  $\tau = 3.6 \times 10^{-1} \text{s}^{-1}$ ) compared to the final stage (4  $\mu\text{M}$  Magainin 2/calcein,  $\tau = 5.6 \times 10^{-2} \text{s}^{-1}$ ) (see table 1 in Ref. [65]). The radius of the pore decreases, and finally, smaller pores become stable. It has also been found that magainin-induced pore formation does not depend significantly on the type of fluorescence probe used. The rate constants for NK-2 obtained from phase contrast microscopy and for Magainin 2 obtained from fluorescence microscopy for different peptide concentrations are summarised in Table 3.

## 4 Mechanisms of pore formation

Antimicrobial peptides are a unique and diverse group of molecules that show different mechanisms of their antimicrobial activity depending on their amino acid composition, amphipathicity, cationic charge, size, sequence, conformation, and structure. Therefore, the mechanisms of antimicrobial activity, i.e., how peptides damage or kill microorganisms, need to be elucidated. Although there are no unique mechanisms for membrane disruption, transmembrane pore formation seems to be a common feature of all the different modes of action of AMPs. Based on the experimental and simulation studies, ‘barrel-stave’, ‘carpet’, and ‘toroidal-pore’ mechanisms are proposed for defining the antimicrobial activity of AMPs [1, 7]. The process of antimicrobial peptide-mediated cell killing begins with the electrostatic attraction of cationic peptides towards negatively charged membranes. Studies based on model membranes show that cationic peptides, such as NK-2, magainin, melittin, cecropin A, and many others, have a strong binding affinity towards anionic phospholipids [35, 46, 54, 61, 69]. Similarly, cationic peptides are

**Table 3** Rate constant or time constant ( $\tau$ ) of the kinetics of pore formation induced by AMPs for different lipid and peptide compositions

Lipids	Peptides	Peptide concentration $\mu\text{M}$ , P/L	$\tau$ ( $\text{sec}^{-1}$ )	References
DOPC/DOPG	NK-2	0.45	0.007	[35]
	NK-2	0.9	0.01	[35]
	NK-2	0.45	0.03	[35]
DOPC/DOPG	Maiganin 2	7	0.014	[69]
	Magainin 2	4	0.059	[65]
DMPC	18D	60	0.0056	[71]
DMPG	18D	60	0.0031	[71]

**Table 4** Model elucidating the mechanisms of antimicrobial activity, i.e., antimicrobial peptide killing and cell lysis [1, 7] (references therein)

Model for transmembrane pore forming mechanisms	Name of peptides
Carpet	Melittin, Cecropin, Dermaseptin S, Caerin and Ovispirin, Human cathelicidin LL-37
Barrel stave (helical-bundle mode)	Alamethicin, Hairpin, Protegrin-1
Toroidal pore (wormhole, disk)	Protegrin, Magainin, Melittin, LL-3765 and MSI-78 lactacin Q, Arenicin

likely to be attracted to the net negative charges that exist on the outer surface of the Gram negative and Gram positive bacteria. Bacterial membrane possesses net negative charges due to the presence of anionic phospholipids and phosphate groups on lipopolysaccharide (LPS) and teichoic acids [72]. A little is known about the interaction of peptides with the LPS [73]. This interaction is indeed important, as peptides need to traverse the capsular polysaccharides before they associate with the outer membrane of the bacteria.

Peptides interact with the lipid bilayer once they access the cytoplasmic membrane of bacteria. At low peptide-to-lipid ratios ( $P/L < P/L^*$ ), different peptides adopt their conformation changes to  $\alpha$ -helix,  $\beta$ -sheet, and  $\theta$ -defensins and embed into the head group of the region lying parallel to the membrane surface ( $S$  state). In vitro model membrane studies have shown such conformational changes and orientation for  $P/L < P/L^*$  [24, 38, 54, 57]. At this stage, peptides also stretch the membrane, as seen from the membrane thinning effect in an oriented multilayer as well as the increase in area in GUV [37] already discussed in Sect. 2.2. With the increase in  $P/L$ , peptides start to reorient perpendicular to the membrane surface (I-state). At sufficiently high  $P/L$  ( $\geq P/L^*$ ), peptides insert into the bilayer, and eventually transmembrane pores are formed. In this stage,  $P/L$  varies with both peptide and lipid compositions [26]. Several models have been proposed to illustrate membrane permeabilization and disintegration (see Table 4).

*Carpet model and detergent-like membrane disruption:* In this model, peptides are electrostatically attracted to anionic phospholipid head groups. Peptides then associate and orient parallel to the membrane, covering the membrane surface in a carpet-like manner (see Fig. 5a). A list of peptides mentioned in Table 4 show their antimicrobial activity through this mechanism. Beyond the threshold or critical concentration of peptide, surface-oriented peptides are known to disintegrate the bilayer in a detergent-like manner, eventually leading to the formation of micelles (Fig. 5d). Although most of the peptides, such as melittin, cecropin, ovispirin, etc., are in an  $\alpha$ -helical conformation while accumulating on the membrane [46, 74], human cathelicidin LL-37 adopts a  $\beta$ -sheet structure but uses carpet-like mechanisms to disrupt the membrane [75]. At a critical threshold concentration, the peptides form toroidal transient pores in the bilayer membrane and then disrupt the membrane, forming micelles after destroying the bilayer curvature.

*Barrel Stave model:* In this model, beyond the threshold of  $P/L$ , peptide helices reorient from S-state to I-state and insert into the hydrocarbon core region in the form of a bundle with a central lumen, much like a barrel made up of helical peptides as the staves [76] and hence the name barrel stave model. The model is depicted in Fig. 5b. As presented in Table 4, alamethicin induces the transmembrane pores of this type. Alamethicin adopts an  $\alpha$ -helical configuration, attaches to, aggregates, and inserts into hydrated oriented bilayers, as revealed from oriented circular dichroism, neutron scattering, and synchrotron X-ray scattering [76, 77]. In this model, the hydrophobic peptide regions align with the hydrocarbon core of the bilayer, and the hydrophilic peptide regions constitute the interior region of the pore, as shown in Fig. 5b. Besides hairpin, protegrin-1 can create stable octameric  $\beta$ -barrels and tetrameric arcs (half barrels) in implicit and explicit membranes by simulations [78].

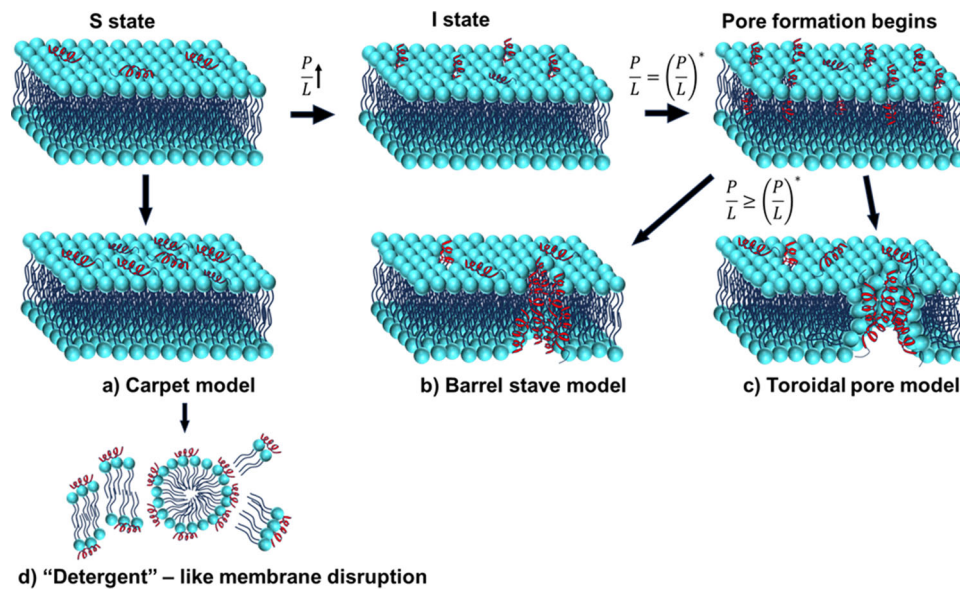


**Fig. 5** Models for antimicrobial peptide-mediated membrane disruption **a** carpet model; **b** Barrel Stave model, **c** toroidal pore model, **d** detergent-like membrane disintegration forms micelles

*Toroidal pore:* Figure 5c shows pore formation by using the toroidal model, also known as the wormhole model. In this model, AMP helices insert into the membrane core, which induces lipid monolayers to bend continuously through the pore so that both the inserted peptide and the lipid head group are exposed to the water column, as depicted in Fig. 5c [79]. A number of peptides (see table 4), such as Magainin, Protegrin, Melittin, LL-3765 and MSI-78, lactacin Q, and arenicin, use this mechanism to form transmembrane pores [75, 78]. The toroidal pore region is lined by both peptide helices and lipid head groups, which are likely to screen and mask cationic peptide charges [76]. Toroidal pores differ from the Barrel stave model from the fact that peptides are always exposed to the lipid head group within the pore region.

All these models discussed above are based on the formation of ion channels, transmembrane pores, and extensive membrane rupture, leading to microbial cell death. However, there is increasing speculation and evidence that these effects are not the only mechanisms of microbial killing. A number of studies indicate that antimicrobial peptides have other non-membrane intracellular targets, much like the action of conventional antibiotics. Non-membrane targeting of AMP will not be discussed in this review. However, readers can find details of antimicrobial activity with non-membrane targets in Refs. [1, 7] and references therein.

## 5 Structural characteristics of pores

The structure of pores is determined from scattering experiments such as neutron scattering [76], synchrotron-based X-ray scattering from oriented bilayer stacks [76], and oriented circular dichroism [26]. These scattering studies estimated the alamethicin-induced transmembrane pores with the inner and outer diameters as  $\sim 1.8$  nm and  $\sim 4.0$  nm, respectively, which contain 3–11 parallel helical molecules. The diameter of the alamethicin helix matches the dimension of the walls of the channel ( $\sim 1.1$  nm). This confirms that alamethicin forms pores according to the barrel stave model, in which eight alamethicin monomers are arranged within the pores [80]. Magainin-induced toroidal pores have an inner diameter of 3.0–5.0 nm and an outer diameter of 7.0–8.4 nm. These pores are larger and have a more variable pore size than alamethicin-induced barrel stave pores. Each pore seems to contain only 4–7 magainin monomers and  $\sim 90$  lipid molecules [76]. The molecular dynamic simulation study [81] also determines the characteristics of pores and estimates the pore size of melittin ( $\sim 1.2$  nm), which is in agreement with the pore size determined from the scattering experiment. Pore size estimation induced by various membrane-active antimicrobial peptides using fluorescence leakage experiments is summarised in a recent review [82], and references therein).

## 6 Advances on the use of AMPs as peptide antibiotics

Studies on the interaction of AMP with lipid membranes have drawn significant attention due to their potential for biomedical applications [2, 83]. The widespread distribution of AMP provides insights into the innate defensive systems that allow the successful evolution of multicellular organisms, including animals and plants, including humans. Diverse applications of AMP as anti-infective agents, anticancer agents, drug delivery, and non-viral gene transfer have led to a large number of studies in view of developing anti-infective drugs. The problems that have impeded the development of drug design are the toxicity and hemolytic effect, i.e., AMPs can kill the cell membranes of eukaryotes. NK-2, a cationic AMP, can have the potential for designing antibiotics, as they are found to be nontoxic and nonhemolytic to human skin cells [84]. As already established, the NK-2 has potential for developing therapeutics to kill the malaria parasite *Plasmodium falciparum* [85]. It also exhibits activity against *Escherichia coli* and preferentially kills cancer cells [86]. A list of applications of AMPs in various fields, including medicine, food, husbandry, and agriculture, is presented in Ref. [7].

$\alpha$ -defensins HNP-1, HNP-2, and HNP-3 exhibited effective antibacterial activity against human papilloma virus, adenovirus, influenza virus, cytomegalovirus, and herpes virus [87]. There has been a recent development in the use of AMPs in the treatment of dental, surgical, and eye infections and wound healing. For example, peptides such as ZXR-2 (FKIGGFIKKLWRSLLA) have shown potent activities against pathogenic bacteria that cause dental caries and cavities [88]. Several AMPs, such as PXL150, have shown pronounced efficacy as an anti-infective agent in burn wounds in mice, and D2A21 is in the third phase of clinical trials for treating burn wound infections [89]. Some AMPs have been found to have possibilities for use as anti-infective therapeutics in the field of ophthalmology [90]. For example, lactoferricin B and protegrin-1 exhibited antimicrobial activity against some pathogenic bacteria, causing eye infections. However, drug preparation in the field of ophthalmology is only at the beginning stage. The development and challenges of antimicrobial peptides for therapeutic applications have been described in a recent review article by Chen et al. [91]. Various local environmental factors, such as enzyme precursor drug release systems and pH, which may trigger or inhibit the antimicrobial activity of AMPs, need to be elucidated to develop AMPs as alternatives to antibiotics. Further, the interaction of these AMPs with the drug delivery agents also needs to be investigated to find efficient and appropriate delivery agents. For instance, nanotubes, quantum dots, graphene, metal nanoparticles, vesicles, etc. have been proposed as potential carriers of drug delivery of AMPs [92].

## 7 Concluding remarks

Antimicrobial peptides are good alternatives for combating drug-resistant bacterial infections as they target the membrane directly for the destruction of invading pathogens. However, the major challenges that have impeded the development of AMPs as drug therapeutics are their short half-lives. AMPs are prone to hydrolysis, oxidation, and photolysis in the microenvironment, such as alkaline pH and proteolysis [3, 4, 93]. Further, most of the AMPs are haemolytic and cytotoxic to non-infected, targeted cells, which may lead to chronic inflammatory diseases. The complexity of the microenvironment led to difficulty in their clinical testing. Therefore, prolonged and expensive clinical research to overcome the above-mentioned unfavourable environment leads to low investment returns. Although it is well established that bacteria are incapable of evolving resistance against AMPs, some recent research suggests that gene mutations can facilitate better survival of the bacteria inside the host cell, indicating the evolution of resistance against AMPs [3]. To overcome the limitations and drawbacks, the latest methods and strategies have been employed, which include the use of composite AMPs to treat drug-resistant bacterial infections ([3] and references therein). The nanoencapsulation of AMPs using metal, polymeric, and lipid nanosystems can protect the peptide from degradation and toxicity. Further, changing the amino acid structure and content can also solve the issue of the drug's toxicity and instability [6]. These strategies provide opportunities to develop more targeted and effective therapies for infectious and cancer diseases. Further research is underway to optimise the properties of composite and modified AMPs and to evaluate their safety and efficacy.

**Acknowledgements** SD acknowledges UGC, Govt. of India for providing fellowship and KKB thanks to Govt of West Bengal for State Fellowship.

**Data availability** Data sharing is not applicable to this article as no new data were created or analyzed in this study.

## References

1. K.A. Brogden, Antimicrobial peptides: pore formers or metabolic inhibitors in bacteria? *Nat. Rev. Microbiol.* **3**, 238–250 (2005)
2. M. Zasloff, Antimicrobial peptides of multicellular organisms. *Nature* **415**, 389–395 (2002)
3. J. Xuan, W. Feng, J. Wang, R. Wang, B. Zhang, L. Bo, Z.-S. Chen, H. Yang, L. Sun, Antimicrobial peptides for combating drug-resistant bacterial infections. *Drug Resist. Updates* **68**, 100954 (2023)
4. M. Mahlapuu, C. Bjorn, J. Ekblom, Antimicrobial peptides as therapeutic agents: opportunities and challenges. *Crit. Rev. Biotechnol.* **40**, 978–992 (2020)
5. P. Kumar, J.N. Kizhakkedathu, S.K. Straus, Antimicrobial peptides: diversity, mechanism of action and strategies to improve the activity and biocompatibility in vivo. *Biomolecules* **8**, 4 (2018)
6. A.A. Bahar, D. Ren, Antimicrobial peptides. *Pharmaceuticals* **6**, 1543–1575 (2013)
7. Y. Huan, Q. Kong, H. Mou, H. Yi, Antimicrobial peptides: classification, design, application and research progress in multiple fields. *Front. Microbiol.* **11**, 2559 (2020)
8. Y. Shai, Antimicrobial peptides: a lesson from nature for future antibiotics. *J. Pept. Sci.* **10**, 112 (2004)
9. Y. Lai, A.E. Villaruz, M. Li, D.J. Cha, D.E. Sturdevant, M. Otto, The human anionic antimicrobial peptide dermcidin induces proteolytic defence mechanisms in staphylococci. *Mol. Microbiol.* **63**, 497–506 (2007)
10. B.B. Finlay, R.E. Hancock, Can innate immunity be enhanced to treat microbial infections? *Nat. Rev. Microbiol.* **2**, 497–504 (2004)
11. R.E. Hancock, A. Patrzykat, Clinical development of cationic antimicrobial peptides: from natural to novel antibiotics. *Curr. Drug Targets Infect. Disord.* **2**, 79–83 (2002)
12. H. Boman, Peptide antibiotics and their role in innate immunity. *Annu. Rev. Immunol.* **13**, 61–92 (1995)
13. M.J. Hope, M.B. Bally, G. Webb, P.R. Cullis, production of large unilamellar vesicles by a rapid extrusion procedure: characterization of size distribution, trapped volume and ability to maintain a membrane potential. *Biochim. Biophys. Acta* **812**, 55–65 (1985)
14. T. Pott, H. Baurrais, P. Meleard, Giant unilamellar vesicles formation under physiologically relevant conditions. *Chem. Phys. Lipids* **154**, 115–119 (2008)
15. A. Baeriswyl, B.-H. Gan, T.N. Siriwardena, R. Visini, M. Robadey, S. Javor, A. Stocker, T. Darbre, J.-L. Reymond, X-ray crystal structures of short antimicrobial peptides as *Pseudomonas aeruginosa* lectin b complexes. *ACS Chem. Biol.* **14**(4), 758–766 (2019)
16. K. Lohner, E.J. Prenner, Differential scanning calorimetry and x-ray diffraction studies of the specificity of the interaction of antimicrobial peptides with membrane-mimetic systems. *Biochim. Biophys. Acta Biomembr.* **1462**(4), 141–156 (1999)
17. D. Gidalevitz, I. Yuji, A.S. Muresan, O. Konovalov, A.J. Waring, R.I. Lehrer, K.Y. Lee, Interaction of antimicrobial peptide protegrin with biomembranes. *Proc. Natl. Acad. Sci. USA* **100**(11), 6302–6307 (2003)
18. B. Bechinger, E.S. Salnikow, The membrane interactions of antimicrobial peptides revealed by solid-state nmr spectroscopy. *Phys. Chem. Lipids* **165**, 281–301 (2012)
19. T. Won, S.A. Mohid, J. Choi, M. Kim, J. Krishnamoorthy, I. Biswas, A. Bhunia, D. Lee, The membrane interactions of antimicrobial peptides revealed by solid-state nmr spectroscopy. *Biophys. Chem.* **296**, 106981 (2023)
20. A. Lorin, M. Noe, M.E. Provencher, V. Turcotte, S. Cardinal, P. Lague, N. Voyer, M. Auger, Determining the mode of action involved in the antimicrobial activity of synthetic peptides: a solid-state nmr and ftir study. *Biophys. J.* **103**, 1470–1479 (2012)
21. N. Sitaram, R. Nagaraj, Interaction of antimicrobial peptides with biological and model membranes: structural and charge requirements for activity. *Biophys. Biochim. Acta* **1462**, 29–54 (1999)
22. M. He, T. Wu, S. Pan, X. Xu, Antimicrobial mechanism of flavonoids against *Escherichia coli* atcc 25922 by model membrane study. *Appl. Surf. Sci.* **305**, 515–521 (2014)
23. A. Roy, N.K. Saragi, S. Ghosh, A. Prabhakaran, T.E. Keyes, Leaflet by leaflet synergistic effects of antimicrobial peptides on bacterial and mammalian membrane models. *J. Phys. Chem. Lett.* **14**, 2920–2928 (2023)
24. C. Olak, A. Muentner, J. Andra, G. Brezesinski, Interfacial properties and structural analysis of the antimicrobial peptide nk-2. *J. Pept. Sci.* **14**, 510–517 (2008)
25. B. Ding, L. Soblosky, K. Nguyen, J. Geng, X. Yu, A. Ramamoorthy, Z. Chen, Physiologically-relevant modes of membrane interactions by the human antimicrobial peptide, LL-37, revealed by sfg experiments. *Sci. Rep.* **3**(1), 1854 (2013)
26. M.-T. Lee, F.-Y. Chen, H.W. Huang, Energetics of pore formation induced by membrane active peptides. *Biochemistry* **43**, 3590–3599 (2004)
27. N. Calderón-Rivera, J. Múnera-Jaramillo, S. Jaramillo-Berrio, E. Suesca, M. Manrique-Moreno, C. Leidy, Cardiolipin strongly inhibits the leakage activity of the short antimicrobial peptide atra-1 in comparison to ll-37, in model membranes mimicking the lipid composition of *Staphylococcus aureus*. *Membranes* **13**, 304 (2023)
28. J. Seelig, Thermodynamics of lipid-peptide interactions. *Biochim. Biophys. Acta* **1666**, 40–50 (2004)
29. M.R. Wenk, J. Seelig, Magainin 2 amide interaction with lipid membranes: calorimetric detection of peptide binding and pore formation. *Biochemistry* **37**, 3909–3916 (1998)
30. T.M. Domingues, B. Mattei, J. Seelig, K.R. Perez, A. Miranda, K.A. Riske, Interaction of the antimicrobial peptide gomesin with model membranes: a calorimetric study. *Langmuir* **29**, 8609–8618 (2013)



31. R. Willumeit, M. Kumpugdee, S.S. Funari, K. Lohner, B.P. Navas, K. Brandenburg, S. Linser, J. Andra, Structural rearrangement of model membranes by the peptide antibiotic nk-2. *Biochim. Biophys. Acta* **1669**, 125–134 (2005)
32. H. Sato, J.B. Feix, Peptide-membrane interactions and mechanisms of membrane destruction by amphipathic  $\alpha$ -helical antimicrobial peptides. *Biochim. Biophys. Acta* **1758**, 1245–1256 (2006)
33. S. Karmakar, P. Maity, A. Halder, Charge-driven interaction of antimicrobial peptide nk-2 with phospholipid membranes. *ACS Omega* **2**, 8859–8867 (2017)
34. T. Salditt, S. Li, A. Spaar, Structure of antimicrobial peptides and lipid membranes probed by interface-sensitive x-ray scattering. *Biochim. Biophys. Acta* **1758**, 1483–1498 (2006)
35. A. Halder, S. Karmakar, An evidence of pores in phospholipid membrane induced by an antimicrobial peptide nk-2. *Biophys. Chem.* **282**, 106759 (2022)
36. M.M. Billah, M.M.O. Rashid, M. Ahmed, M. Yamazaki, Antimicrobial peptide magainin 2-induced rupture of single giant unilamellar vesicles comprising *E. coli* polar lipids. *Biochim. Biophys. Acta Biomembr.* **1865**, 184112 (2023)
37. M.Z. Islam, J.M. Alam, Y. Tamba, M.A.S. Karal, M. Yamazaki, The single guv method for revealing the functions of antimicrobial, pore-forming toxin, and cell-penetrating peptides or proteins. *Phys. Chem. Chem. Phys.* **16**, 15752–15767 (2014)
38. M.-T. Lee, T.-L. Sun, W.-C. Hung, H.W. Huang, Process of inducing pores in membranes by melittin. *Proc. Natl. Acad. Sci. USA* **110**, 14243–14248 (2013)
39. M. Nithya, B.R. Vincent, O. Sarangi, V. Kumar, Kinetics of nisin-induced pore formation in giant unilamellar vesicles. *Langmuir* **39**, 11231–11237 (2023)
40. A.D. Cirac, G. Moisset, J.T. Mika, A. Kocer, P. Salvador, B. Poolman, S.J. Marrink, D. Sengupta, The molecular basis for antimicrobial activity of pore-forming cyclic peptides. *Biophys. J.* **100**, 2422–2431 (2011)
41. I.S. Tolokh, V. Vivcharuk, B. Tomberli, C.G. Gray, Binding free energy and counterion release for adsorption of the antimicrobial peptide lactoferricin b on a popg membrane. *Phys. Rev. E* **80**, 031911 (2009)
42. C.I.E. von Deuster, V. Knecht, Antimicrobial selectivity based on zwitterionic lipids and underlying balance of interactions. *Biochim. Biophys. Acta* **1818**, 2192–2201 (2012)
43. A. Arouri, M. Dathe, A. Blume, Peptide induced demixing in pg/pe lipid mixtures: a mechanism for the specificity of antimicrobial peptides towards bacterial membranes? *Biochim. Biophys. Acta* **1788**, 650–659 (2009)
44. G.J. Gabriel, J.G. Pool, A. Som, J.M. Dabkowski, E.B. Coughlin, M. Muthukumar, G.N. Tew, Interactions between antimicrobial polynorbornenes and phospholipid vesicles monitored by light scattering and microcalorimetry. *Langmuir* **24**, 12489–12495 (2008)
45. M.L. Chen, R.L. Johnson, A. Biltonen, A macroscopic description of lipid bilayer phase transitions of mixed-chain phosphatidylcholines: chain-length and chain asymmetry dependence. *Biophys. J.* **80**, 254–270 (2001)
46. B. Bechinger, Structure and functions of channel-forming peptides: magainins, cecropins, melittin and alamethicin. *J. Membr. Biol.* **156**, 197–211 (1997)
47. Y. Chen, M.T. Guarnieri, A.I. Vasil, M.L. Vasil, C.T. Mant, R.S. Hodges, Role of peptide hydrophobicity in the mechanism of action of  $\alpha$ -helical antimicrobial peptides. *Antimicrob. Agents Chemother.* **51**, 1398–1406 (2007)
48. L.M. Yin, M.A. Edwards, J. Li, C.M. Yip, C.M. Deber, Roles of hydrophobicity and charge distribution of cationic antimicrobial peptides in peptide-membrane interactions. *J. Biol. Chem.* **287**, 7738–7745 (2012)
49. M.-A. Sani, F. Separovic, How membrane-active peptides get into lipid membranes. *Acc. Chem. Res.* **49**, 1130–1138 (2016)
50. T. Tachi, R.F. Epand, R.M. Epand, K. Matsuzaki, Position-dependent hydrophobicity of the antimicrobial magainin peptide affects the mode of peptide-lipid interactions and selective toxicity. *Biochemistry* **41**, 10723–10731 (2002)
51. M. Bastos, O. Abian, C.M. Johnson, F. Ferreira-da-Silva, S. Vega, A. Jimenez-Alesanco, D. Ortega-Alarcon, V. Velazquez-Campoy, Isothermal titration calorimetry. *Nat Rev Methods Prim.* **3**(17) (2023)
52. T. Wierprecht, O. Apostolov, M. Beyermann, J. Seelig, Membrane binding and pore formation of the antibacterial peptide pglA. *Biochemistry* **39**(2), 442–452 (2000)
53. H. Binder, G. Lindblom, Charge-dependent translocation of the trojan peptide penetration across lipid membranes. *Biophys. J.* **85**, 982–995 (2003)
54. M.-T. Lee, W.-C. Hung, F.Y. Chen, H.W. Huang, Mechanism and kinetics of pore formation in membranes by water-soluble amphipathic peptides. *Proc. Natl. Acad. Sci. USA* **105**, 5087–5092 (2008)
55. K. Matsuzaki, S. Yoneyama, K. Miyajima, Pore formation and translocation of melittin. *Biophys. J.* **73**, 831–838 (1997)
56. S.A. Akimov, P.E. Volynsky, T.R. Galimzyanov, P.I. Kuzmin, K.V. Pavlov, O.V. Batishev, Pore formation in lipid membrane II: energy landscape under external stress. *Sci. Rep.* **7**, 12509 (2017)
57. H.W. Huang, Action of antimicrobial peptides: two-state model. *Biochemistry* **39**, 8347–8352 (2000)
58. P.E. Volynsky, A.A. Polyansky, N.A. Simakov, A.S. Arseniev, R.G. Efremov, Effect of lipid composition on the “membrane response” induced by a fusion peptide. *Biochemistry* **44**, 14626–14637 (2005)
59. N.H. Wubshet, A.P. Liu, Methods to mechanically perturb and characterize guv-based minimal cell models. *Comput. Struct. Biotechnol. J.* **21**, 550–562 (2023)
60. H.W. Huang, F.-Y. Chen, M.-T. Lee, Molecular mechanism of peptide-induced pores in membranes. *Phys. Rev. Lett.* **92**, 198304 (2004)
61. T. Benachir, M. Monette, J. Grenier, M. Lafleur, Melittin-induced leakage from phosphatidylcholine vesicles is modulated by cholesterol: a property used for membrane targeting. *Eur. Biophys. J.* **25**, 201–210 (1997)

62. A. Halder, A. Sannigrahi, N. De, K. Chattopadhyay, S. Karmakar, Kinetoplastid membrane protein-11 induces pores in anionic phospholipid membranes: effect of cholesterol. *Langmuir* **36**, 3522–3530 (2020)
63. J. Oñate-Garzón, M. Manrique-Moreno, S. Steven Trier, C. Leidy, R. Torres, E. Patino, Antimicrobial activity and interactions of cationic peptides derived from galleria mellonella cecropin d-like peptide with model membranes. *J. Antibiot.* **70**, 238–245 (2017)
64. A. Tuerkova, I. Kabelka, T. Králová, L. Sukeník, S. Pokorná, M. Hof, S. Vácha, Effect of helical kink in antimicrobial peptides on membrane pore formation. *eLife* **9**, e47946 (2020)
65. Y. Tamba, M. Yamazaki, Single giant unilamellar vesicle method reveals effect of antimicrobial peptide magainin 2 on membrane permeability. *Biochemistry* **44**, 15823–15833 (2005)
66. A. Mularski, J.J. Wilksch, E. Hanssen, R.A. Strugnell, F. Separovic, Atomic force microscopy of bacteria reveals the mechanobiology of pore forming peptide action. *Biochim. Biophys. Acta* **1858**, 1091–1098 (2016)
67. A. Farkas, G. Maroti, A. Kereszt, E. Kondorosi, Comparative analysis of the bacterial membrane disruption effect of two natural plant antimicrobial peptides. *Front Microbiol.* **8**(4), 51 (2017)
68. E.H.-L. Chen, C.-H. Wang, Y.-T. Liao, F.-Y. Chan, Y. Kanaoka, T. Uchihashi, K. Kato, L. Lai, Y.-W. Chang, M.-C. Ho, R.P.-Y. Chen, Visualizing the membrane disruption action of antimicrobial peptides by cryo-electron tomography. *Nat Commun.* **14**, 5464 (2023)
69. Y. Tamba, H. Ariyama, V. Levandy, M. Yamazaki, Kinetic pathway of antimicrobial peptide magainin 2-induced pore formation in lipid membranes. *J. Phys. Chem. B* **114**, 12018–12026 (2010)
70. Y. Tamba, M. Yamazaki, Magainin 2-induced pore formation in the lipid membranes depends on its concentration in the membrane interface. *J. Phys. Chem. B* **113**, 4846–4852 (2009)
71. H. Mozsolitis, T.H. Lee, A.H.A. Clayton, W.H. Sawyer, M.I. Aguilar, The membrane-binding properties of a class amphipathic peptide. *Eur. Biophys. J.* **33**, 98–108 (2004)
72. H. Strahl, J. Errington, Bacterial membranes: structure, domains, and function. *Annu. Rev. Microbiol.* **71**, 519–538 (2017)
73. L. Ding, L. Yang, T.M. Weiss, A.J. Waring, R.I. Lehrer, H.W. Huang, Interaction of antimicrobial peptides with lipopolysaccharides. *Biochemistry* **42**, 12251–12259 (2003)
74. S. Yamaguchi, D. Huster, A. Waring, R.I. Lehrer, W. Kearney, B.F. Tack, M. Hong, Orientation and dynamics of an antimicrobial peptide in the lipid bilayer by solid-state nmr spectroscopy. *Biophys. J.* **81**, 2202–2214 (2001)
75. Z.O. Shenkarev, S.V. Balandin, K.I. Trunov, A.S. Paramonov, S.V. Sukhanov, L.I. Barsukov, A.S. Arseniev, T.V. Ovchinnikova, Molecular mechanism of action of  $\beta$ -hairpin antimicrobial peptide arenicin: oligomeric structure in dodecylphosphocholine micelles and pore formation in planar lipid bilayers. *Biochemistry* **50**, 6255–6265 (2011)
76. T.A.L. Yang, W. Harroun, T.M. Ding, L. Ding, H.W. Huang, Barrel-stave model or toroidal model? A case study on melittin pores. *Biophys. J.* **81**, 1475–1485 (2001)
77. A. Spaar, C. Munster, T. Salditt, Conformation of peptides in lipid membranes studied by x-ray grazing incidence scattering. *Biophys. J.* **87**, 396–407 (2004)
78. R.B. Lipkin, T. Lazaridis, Implicit membrane investigation of the stability of antimicrobial peptide  $\beta$ -barrels and arcs. *Biophys. J.* **248**, 469–486 (2015)
79. K. Matsuzaki, O. Murase, N. Fujii, K. Miyajima, R.B. Lipkin, T. Lazaridis, An antimicrobial peptide, magainin 2, induced rapid flip-flop of phospholipids coupled with pore formation and peptide translocation. *Biochemistry* **35**, 11361–11368 (1996)
80. K. He, S.J. Ludtke, D.L. Worcester, H.W. Huang, Neutron scattering in the plane of membranes: structure of alamethicin pores. *Biophys. J.* **70**, 2656–2666 (1996)
81. D. Sengupta, H. Leontiadou, A.E. Mark, S.-J. Marrink, Toroidal pores formed by antimicrobial peptides show significant disorder. *Biochim. Biophys. Acta* **1778**, 2308–2317 (2008)
82. B. Bertrand, R. Garduo-Juárez, C. Munoz-Garay, Estimation of pore dimensions in lipid membranes induced by peptides and other biomolecules: a review. *Curr. Pharm.* **1863**, 183551 (2021)
83. N. Stempel, J. Strehmel, J. Overhage, Potential application of antimicrobial peptides in the treatment of bacterial biofilm infections. *Curr. Pharm.* **21**, 67–84 (2015)
84. J. Andra, M. Leippe, Candidacidal activity of shortened synthetic analogs of amoebapores and nk-lysin. *Med. Microbiol. Immunol.* **188**, 117–2317 (1999)
85. J. Andra, M. Leippe, The antimicrobial peptide nk-2, the core region of mammalian nk-lysin, kills intraerythrocytic plasmodium falciparum. *Antimicrob. Agent Chemother.* **52**, 1713–1720 (2008)
86. H. Schröder-Borm, R. Bakalova, J. Andrä, The nk-lysin derived peptide nk-2 preferentially kills cancer cells with increased surface levels of negatively charged phosphatidylserine. *FEBS Lett.* **579**, 6128–6134 (2005)
87. C. de la Fuente-Núñez, O.N. Silva, T.K. Lu, O.L. Franco, Antimicrobial peptides: role in human disease and potential as immunotherapies. *Pharmacol. Ther.* **178**, 132–140 (2017)
88. L. Chen, L. Jia, Q. Zhang, X. Zhou, Z. Liu, B. Li, Z. Zhu, F. Wang, C. Yu, Q. Zhang, F. Chen, S.-Z. Luo, A novel antimicrobial peptide against dental-caries-associated bacteria. *Anaerobe* **47**, 165–172 (2017)
89. C. Björn, L. Noppa, E.N. Salomonsson, A.-L. Johansson, E. Nilsson, M. Mahlapuu, J. Håkansson, Efficacy and safety profile of the novel antimicrobial peptide pxl150 in a mouse model of infected burn wounds. *Int. J. Antimicrob. Agents* **45**, 519–524 (2015)
90. S.A. Khan, C.-S. Lee, Recent progress and strategies to develop antimicrobial contact lenses and lens cases for different types of microbial keratitis. *Acta Biomater.* **113**, 101–118 (2020)

91. C.H. Chen, T.K. Lu, Development and challenges of antimicrobial peptides for therapeutic applications. *Antibiotics* **9**, 24 (2020)
92. M. Magana, M. Pushpanathan, A.L. Santos, L. Leanse, M. Fernandez, A. Ioannidis, M.A. Giulianotti, Y. Apidianakis, S. Bradfute, A.L. Ferguson, A. Cherkasov, M.N. Seleem, C. Pinilla, C. Fuente-Nunez, T. Lazaridis, T. Dai, R.A. Dai THoughten, R.E.W. Hancock, G.P. Tegos, The value of antimicrobial peptides in the age of resistance. *Lancet Infect. Dis.* **20**, 216–230 (2020)
93. R.K. Thapa, D.B. Diep, H.H. Tønnesen, Topical antimicrobial peptide formulations for wound healing: current developments and future prospects. *Acta Biomater.* **103**, 52–57 (2020)

Springer Nature or its licensor (e.g. a society or other partner) holds exclusive rights to this article under a publishing agreement with the author(s) or other rightsholder(s); author self-archiving of the accepted manuscript version of this article is solely governed by the terms of such publishing agreement and applicable law.